THE JOURNAL OF BIOLOGICAL CHEMISTRY VOL. 282, NO. 13, pp. 9874–9882, March 30, 2007

Heteromeric Assembly of Human Ether-à-go-go-related Gene (hERG) 1a/1b Channels Occurs Cotranslationally via N-terminal Interactions*[S]

Received for publication, November 27, 2006, and in revised form, January 8, 2007 Published, JBC Papers in Press, February 1, 2007, DOI 10.1074/jbc.M610875200

Pallavi Phartiyal[‡§], **Eugenia M. C. Jones**[‡], **and Gail A. Robertson**[‡1]

From the [‡]*Department of Physiology and* [§]*Cellular and Molecular Biology Program, University of Wisconsin, Madison, Wisconsin 53711*

Alternate transcripts of the human ether-à-go-go-related gene (*hERG1*) encode two subunits, hERG 1a and 1b, which form potassium channels regulating cardiac repolarization, neuronal firing frequency, and neoplastic cell growth. The 1a and 1b subunits are identical except for their unique, cytoplasmic N termini, and they readily co-assemble in heterologous and native systems. We tested the hypothesis that interactions of nascent N termini promote heteromeric assembly of 1a and 1b subunits. We found that 1a and 1b N-terminal fragments bind in a direct and dose-dependent manner. hERG1 hetero-oligomerization occurs in the endoplasmic reticulum where co-expression of N-terminal fragments with hERG1 subunits disrupted oligomerization and core glycosylation. The disruption of core glycosylation, a cotranslational event, allows us to pinpoint these N-terminal interactions to the earliest steps in biogenesis. Thus, N-terminal interactions mediate hERG 1a/1b assembly, a process whose perturbation may represent a new mechanism for disease.

Potassium channels encoded by the human ether-à-go-go-related gene (*hERG1*)[2] are important in controlling cardiac excitability, neuronal firing frequency, tumor cell proliferation, and smooth muscle function (1–7). Clinically, they are considered the primary target for acquired long QT syndrome (LQTS) (4, 5, 8) caused when drugs intended for other therapeutic targets block hERG1 channels and trigger catastrophic ventricular arrhythmias and sudden death. Mutations in *hERG1* give rise to congenital LQTS (9). Although only a fraction of the more than 200 potential disease-causing mutations in *hERG* have been analyzed in heterologous expression systems, most reduce surface membrane expression of channels because mutant subunits fail to exit the endoplasmic reticulum (ER) (10–15). Little is known about why such LQTS-2 mutants fail to mature. In theory, maturation defects could result from misfolding, failed oligomeric assembly, or trafficking defects during translocation of channel complexes to the plasma membrane (16, 17). Drugs can rescue a subset of mutants, as if by stabilizing the internal vestibule of the pore and thus compensating for folding or oligomerization defects (18).

We are only beginning to understand how ion channels assemble (19). Studies of certain voltage-gated potassium (Kv) channels and neurotransmitter receptors indicate that assembly of related subunits is specified by N-terminal interactions (20–22). In homomeric Kv1.3 channels, N termini interact as they emerge from the translocon, well before subunit synthesis is complete (23). In contrast to Kv or ligand-gated channels, where homologous N termini mediate association, hERG subunits present an unusual challenge: they exist as two isoforms that are identical except for structurally divergent N termini. The hERG 1a N terminus comprises ~396 residues, whereas the 1b N terminus is a mere 56 residues, the first 36 of which are unique (Fig. 1*A*). The two subunits assemble in native tissues and in heterologous systems (24) where, in the absence of hERG 1a, 1b subunits fail to form robust homomeric currents (25, 26). If the N termini are involved in assembly for hERG channels as for other potassium channels, the underlying mechanisms may differ substantially from those regulating association of homologous domains. Understanding these mechanisms is an important first step to uncovering new determinants of LQTS that occur because of defects in biogenesis.

In this study we tested the hypothesis that cotranslational interactions between the 1a and 1b N termini promote heteromeric subunit association. We show that hERG 1a and 1b N termini interact in cellular and *in vitro* assays. We utilized a truncated 1b subunit, which is retained in the ER, as a reporter of early biogenic events. Homo-oligomers of this subunit are core-glycosylated, but glycosylation can be disrupted by the introduction of heteromerizing 1a N-terminal fragments. Thus, heteromeric interactions occur before the addition of the glycan group in the ER. Such non-homotypic interactions between structurally dissimilar N termini occur cotranslationally and likely function to facilitate the heteromerization of hERG1 channel subunits.

* This work was supported in part by National Institutes of Health Grant R01 HL081780 (to G. A. R.) and an American Heart Association Predoctoral Fellowship (to P. P.). The costs of publication of this article were defrayed in part by the payment of page charges. This article must therefore be hereby marked "*advertisement*" in accordance with 18 U.S.C. Section 1734 solely to indicate this fact.

[S] The on-line version of this article (available at http://www.jbc.org) contains supplemental Figs. S1–S4.

[1] To whom correspondence should be addressed: Dept. of Physiology, University of Wisconsin Satellite Laboratories, 601 Science Dr., Madison, WI 53711. Tel.: 608-265-3339; Fax: 608-265-7821; E-mail: robertson@physiology.wisc.edu.

[2] The abbreviations used are: hERG1, human ether-à-go-go related gene; ER, endoplasmic reticulum; aa, amino acids; TM, transmembrane; GFP, green fluorescent protein; GST, glutathione *S*-transferase; LQTS, long QT syndrome; HEK, human embryonic kidney; IP, immunoprecipitate; Endo H, endoglycosidase H.

EXPERIMENTAL PROCEDURES

Plasmids—For mammalian expression, hERG 1a (aa 1–1159) and 1b (aa 1–819) cDNA were subcloned into pcDNA3.1 vector (Invitrogen). C-terminal-truncated clones, lacking 461 aa of the distal region, 1aΔCT (aa 1–698) and 1bΔCT (aa 1–358), were subcloned into pcDNA3.1/Myc-His vector (Invitrogen). hERG1 N-terminal fragments with the first two transmembrane (TM) domains were subcloned using PCR with a 3′ oligo that introduced a FLAG tag sequence at the end of the second TM (aa 476 for 1a and 136 for 1b). Amplified fragments were cloned into pcDNA3.1 vector and sequenced.

For bacterial expression, 1a N terminus (1aNT, aa 1–367) was cloned into pET28a(+) vector (Novagen) resulting in an N-terminal His tag. The 1b N terminus (1bNT, aa 1–67) was cloned into pGex4T-1 vector (Amersham Biosciences) and bears a GST tag on the N-terminal end. Both pGex4T-1 and pET28a clones were transformed into Rosetta(DE3)pLysS cells (Novagen).

Antibodies—The generation of pan-ERG1 rabbit antibody against the C terminus of hERG1, and 1a and 1b isoform-specific rabbit antibodies has been described previously (24). For Western blotting, the antibodies were used at 1:5000, 1:150, and 1:1000 dilutions, respectively. Mouse anti-c-Myc (Clontech) was used at a dilution of 1:250. Goat anti-1a (Santa Cruz Biotechnology) was used at 1:200 dilution. Mouse pan-hERG1 antisera were produced in collaboration with Neoclone (Madison, WI) and used at 1:500.

Cell Culture—Human embryonic kidney (HEK)-293 cells were cultured in Dulbecco's modified Eagle's medium at 37 °C. A cell line stably expressing 1bΔCT protein was generated by transfecting HEK-293 cells with Myc-tagged 1bΔCT DNA and growing in medium containing 1 mg/ml neomycin for selection. Separate cell colonies were selected, and lysate from them was probed with 1b-specific antibody to confirm expression. Cell lines expressing 1bΔCT were then maintained in 500 μg/ml neomycin.

Protein Expression and Purification from HEK-293 Cells—Cells were transfected with appropriate quantity of DNA at 70–80% confluency using TransIT-LT1 kit (Mirus). Membrane preparations were made, 48 h post-transfection, by solubilizing cells in 150 mM NaCl, 25 mM Tris-HCl, pH 7.4, 20 mM NaEDTA, 10 mM NaEGTA, 5 mM glucose, and 0.5–1% (v/v) Triton X-100 followed by sonication and incubation for 15 min. Lysates were cleared of debris by centrifugation at 10,000 × *g* for 15 min, and the supernatant quantified using the Bradford assay (DC Protein Assay, Bio-Rad). All steps were carried out at 4 °C.

Co-immunoprecipitation—Cell lysates were precleared with 25 μl of 25% protein A/G bead slurry (Amersham Biosciences) for 30 min at 4 °C. Precleared lysate was incubated with respective antibody for 3 h. Lysates were further incubated with 50 μl of 25% protein A/G slurry for 2 h at 4 °C. Protein complexes were collected by centrifugation at 2,000 × *g*. Beads were washed three times in 0.1% Triton X-100 containing solubilization buffer. Immune complexes were eluted in 5× LSB (225 mM Tris-HCl, pH 6.8, 5% SDS, 50% glycerol, 200 mM dithiothreitol) at 65 °C for 5 min. Eluted protein complexes, alongside their input lysate, were size-separated by SDS-PAGE and Western-blotted using standard methods.

Co-immunoprecipitation was used to isolate complexes of the $1aNT_{tm}$ fragment with the truncated 1bΔCT construct in stably expressing 1bΔCT cells to observe the effects of association on 1bΔCT core glycosylation. In contrast, in transient co-transfections the effects could be seen in the lysate without co-immunoprecipitation. We inferred that the inability to observe an effect in stable cell lysates without co-immunoprecipitation is because of the reduced efficiency of co-expression of the two constructs compared with transient transfections in which both constructs are simultaneously introduced and coordinately translated.

Protein Expression and Purification in Escherichia coli—Recombinant proteins were purified as per manufacturer's protocol (Amersham Biosciences and Novagen). Purified 1aNT-His_6 protein was eluted from Ni^{2+} beads (Qiagen) with 250 mM imidazole and desalted and exchanged in 20 mM HEPES, pH 7.4, 500 mM NaCl by Amicon 10K column (Millipore). Purified proteins were size-separated by SDS-PAGE, stained by Coomassie Blue, and quantified by comparison with bovine serum albumin protein standards.

GST Pull-down Assays—Binding assays were carried out by incubating the indicated amounts of soluble 1aNT-His_6 with 2 μM immobilized recombinant fusion proteins, 1bNT or GST. Reactions were incubated with agitation for 2 h at 4 °C in a total volume of 150 μl of TBS buffer containing 0.5% Triton X-100 (binding buffer). Bound proteins were washed three times with 1 ml of binding buffer, and eluted by boiling in LSB. The entire binding reaction was subjected to SDS-PAGE and Coomassie Blue staining.

Endoglycosidase Analysis—Deglycosylation was performed according to the manufacturer's protocol. 8 μg of denatured lysate was treated with either endoglycosidase H (Roche Applied Science) or PNGase F (New England Biolabs) overnight at 37 °C. In control reactions, the enzymes were replaced with buffer.

Pulse Chase—HEK-293 cells were grown to 70% confluency and transfected with 10 μg of 1bΔCT DNA with either 10 μg of $1aNT_{tm}$ or 10 μg of pcDNA3.1 using $Ca_3(PO)_4$ (27). Two days post-transfection, cells were starved for 15 min, pulsed with 250 μCi of ^{35}S Promix (Amersham Biosciences) per dish for 5 min. Cells were chased with unlabeled medium for the indicated times. Cells were suspended in lysis buffer and incubated for 30 min at 4 °C. Radiolabeled lysates were clarified by centrifugation, quantified, and immunoprecipitated with either 1b-specific (for pcDNA3.1-transfected cells) or 1a-specific ($1aNT_{tm}$-transfected cells) antibodies for 3 h, and immune complexes were isolated with protein A beads for 12–16 h at 4 °C. Proteins were eluted with LSB, heated at 65 °C for 5 min, and size-separated by SDS-PAGE. Gels were fixed in a 25% isopropyl alcohol and 10% acetic acid solution, dried at 80 °C for 2 h, and exposed to a phosphorscreen. Pulse chase for 1bΔCT stable cells was set up similarly with indicated pulse and chase times.

Fractional Centrifugation—HEK-293 1bΔCT cells were transfected with DNA for either pcDNA3.1 vector or $1aNT_{tm}$. Cells were homogenized in 750 μl of protease inhibitor (Roche

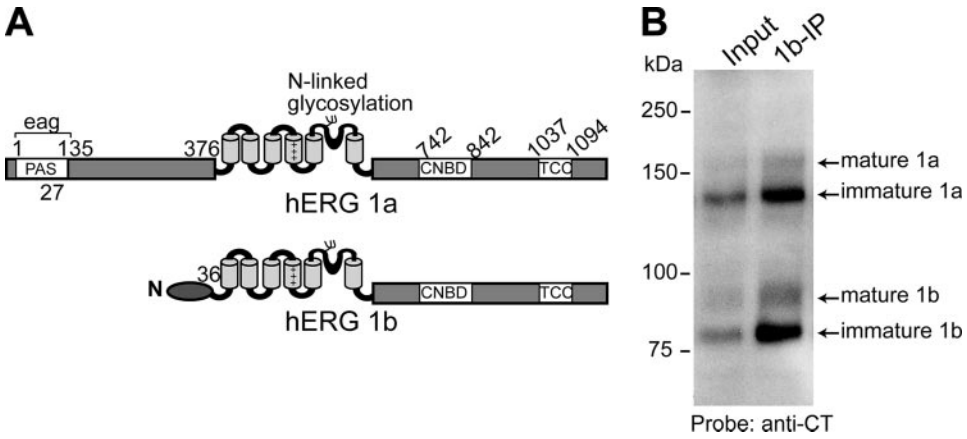

FIGURE 1. **hERG1 subunits assemble in the ER.** *A*, *schematic* illustrating different cytoplasmic N-terminal domains of hERG 1a and 1b. Labels indicate the *N*-linked glycosylation site and protein domains ether-a-go-go (*eag*), Per-Arnt-Sim (*PAS*), putative cyclic nucleotide binding domain (*CNBD*), and tetramerization coiled-coil (*TCC*). *B*, lysate from HEK-293 cells transiently expressing 1a and 1b was immunoprecipitated with 1b-specific rabbit antibody, and the Western blot was probed with mouse antibody against the common C terminus of hERG1 isoforms. The immature species typically dominates in transient transfections. The mature and immature 1a glycoforms migrate at 155 and 135 kDa, respectively. Immature and mature 1b proteins migrate at 85 and 95 kDa, respectively.

minitab)-supplemented 10 mM Tris-HCl, pH 7.4, 250 mM sucrose, 2 days post-transfection. Cells were lysed manually using a 25-gauge needle. Lysate was centrifuged at 1,000 × *g* to remove crude cellular debris (1,000 × *g* pellet). Supernatant was collected and centrifuged at 10,000 × *g* for 30 min to separate large membranes (*e.g.* ER, Golgi, plasma membrane; 10,000 × *g* pellet). The supernatant was subjected to a final centrifugation at 100,000 × *g* for 90 min to separate small organelles (*e.g.* endosomes, lysosomes; 100,000 × *g* pellet) and the cytosol (100,000 × *g* supernatant). Each pellet was dissolved in 300 μl of lysis buffer (protease-inhibitor supplemented 50 mM Tris-HCl, pH 7.2, 1 mM EDTA, 150 mM sodium chloride, 1% Triton X-100). Up to 1% Triton X-100 was added to lyse the cytosolic fraction.

Densitometry and Statistical Analysis—Coomassie Blue-stained gels and x-ray films of Western blots were quantified by measuring optical density using LabWorks Image and Acquisition Analysis Software (Upland, CA). Data were analyzed using PRISM 2.0 software (GraphPad, San Diego).

For *in vitro* binding assays (Fig. 3), data from three separate experiments were normalized, plotted, and fitted with variable slope sigmoidal dose-response Equation 1,

$$Y = \text{Min} + \{(\text{Max} - \text{Min})/[1 + 10^{(\log EC_{50} - X)} \times \text{Hill Slope}]\} \quad \text{(Eq. 1)}$$

where X is the logarithm of concentration and Y is the response.

For assessing the degree of 1bΔCT homo-oligomerization in the absence or presence of the disrupting $1aNT_{tm}$ fragment (Fig. 5), we used the formula in Equation 2.

$$\text{Level of homo-oligomerization} = (\text{1b}\Delta\text{CT-GFP}/\text{1b}\Delta\text{CT-Myc})_{input}/(\text{1b}\Delta\text{CT-GFP}/\text{1b}\Delta\text{CT-Myc})_{IP} \quad \text{(Eq. 2)}$$

This formula allowed us to take in account the variability in 1bΔCT-GFP and 1bΔCT-Myc protein expression in different sets of lysates. Data were analyzed by running column statistics for one-sample Student's *t* test.

For disruption experiments (Fig. 6), optical density (OD) values for core glycosylated/total 1bΔCT from lysates of cells co-transfected with 1bΔCT and each of the disruption fragments were individually compared with the fractional OD value from 1bΔCT+pcDNA3.1 co-transfected lysate. Data from three experiments were analyzed using a Student's unpaired *t* test and a two-tailed *p* value and are presented as mean ± S.E.; *n* indicates the number of experiments.

RESULTS

hERG1 Subunits Assemble in the ER—Core glycosylation of proteins has been shown to be a cotranslational event in the ER lumen (29–31). Subsequently, the glycan groups are further modified in the medial Golgi, rendering fully mature, complexly glycosylated species (32). hERG 1a subunits undergo *N*-linked core glycosylation in the ER at a single site between the S5 transmembrane domain and the P-region (28). We showed previously that hERG 1b subunits expressed in HEK-293 cells mature from an ~85-kDa core-glycosylated species in the ER to a ~90-kDa species in the medial Golgi (24), similar to the maturation process for hERG 1a subunits (33). Here we show both the mature and immature glycoforms of hERG 1a and 1b can be co-immunoprecipitated from cells transiently transfected with the corresponding cDNA (Fig. 1*B*, *lane 2*). The co-immunoprecipitation of immature 1a with 1b subunits indicates they assemble prior to Golgi glycosylation, likely in the ER.

hERG 1a and 1b N Termini Interact in Mammalian Cells—To identify the soluble domains required for channel association, we first tested whether heteromeric interactions were preserved in the absence of the C terminus, which might mediate heteromerization. We found that 1aΔCT and 1bΔCT proteins co-expressed in HEK-293 cells could be co-immunoprecipitated using 1a-specific antibodies (Fig. 2*B*, *lanes 1* and *2*). This association requires interaction of the truncated proteins *in vivo*, because 1aΔCT and 1bΔCT did not associate in mixed lysates independently expressing the two constructs (Fig. 2*B*, *lanes 3* and *4*). We conclude that the C terminus, which includes a tetramerization coiled-coil (TCC) domain (34), is not required for hERG 1a/1b heteromeric association.

To determine whether an intact hydrophobic core is required to mediate association, we made more extensive C-terminal truncations leaving only the N terminus and the first two TM domains ($1aNT_{tm}$ and $1bNT_{tm}$, Fig. 2*C*). Including the first two TMs allows the short N terminus of the 1b subunit to fully emerge from the translocon and attain proper tertiary structure (19). We co-expressed $1aNT_{tm}$ and $1bNT_{tm}$ in HEK-293 cells, and immunoprecipitated the cell lysate with 1a-spe-

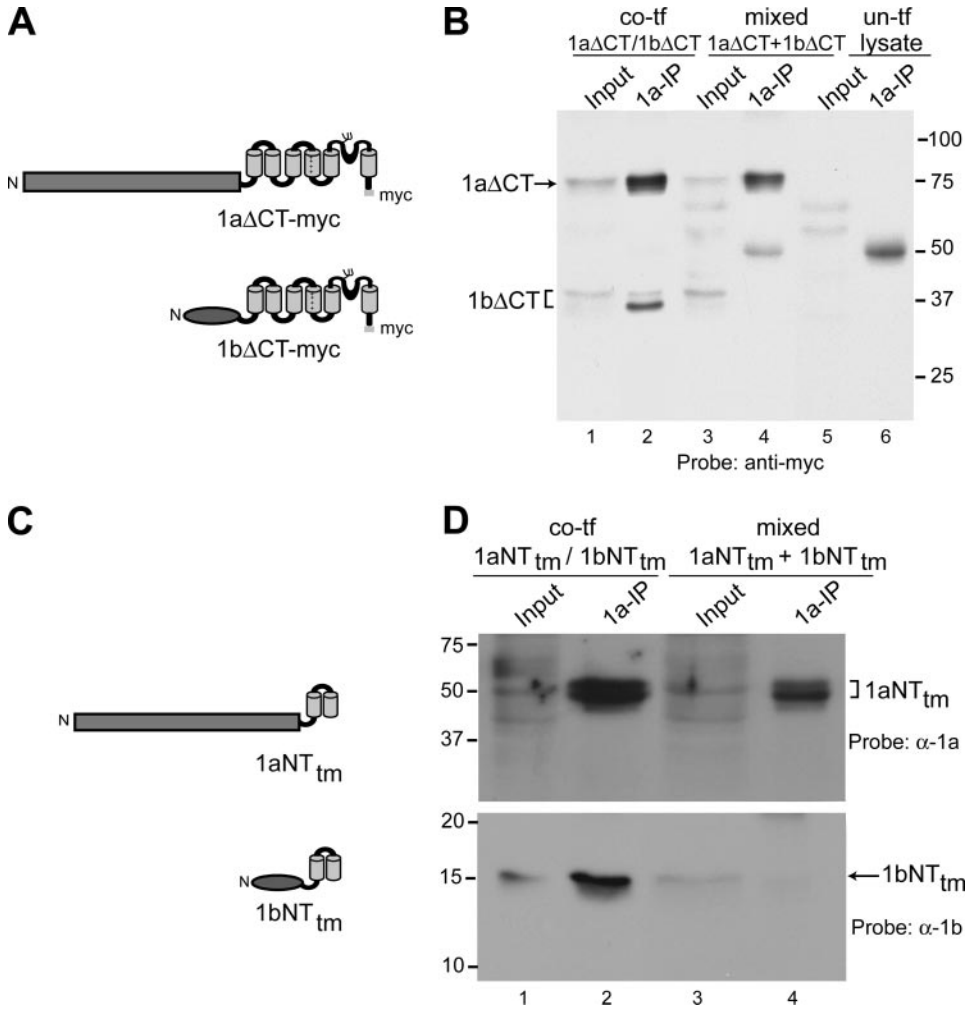

FIGURE 2. **hERG 1a and 1b N termini are sufficient for interaction.** *A*, *schematic* of C-terminal-truncated 1a and 1b subunits. *B*, Western blot probed with Myc antibody. *Lane 1*, cell lysate co-expressing Myc-tagged 1aΔCT and 1bΔCT. *Lane 2*, same lysate immunoprecipitated with 1a-specific antibody. *Lanes 3* and *4*, IPs were ineffectual from mixed lysates independently expressing 1aΔCT and 1bΔCT. *Lanes 5* and *6*, input and IPs from untransfected controls show nonspecific and IgG bands, respectively. Input represents 5% of the total protein used for IP in each case. The entire IP eluate was loaded for each condition. *C*, *schematic* of more extensively truncated 1a and 1b subunits, including only the N termini and the first two TMs. *D*, Western blots probed with 1a antibody (*upper panel*) and 1b antibody (*lower panel*) showing association of $1aNT_{tm}$ and $1bNT_{tm}$. *Lane 1*, input, and *lane 2*, IP using 1a antibody showing association of the two subunits. *Lanes 3* and *4*, mixed lysates independently expressing the two constructs show $1bNT_{tm}$ failed to co-immunoprecipitate with 1a. The inputs represent ~10% of total protein lysate used for IP.

cific antibodies. $1bNT_{tm}$ protein co-precipitated with $1aNT_{tm}$ demonstrating the N termini and first two TMs were sufficient to support association between the 1a and 1b fragments (Fig. 2*D*, *lanes 1* and *2*). As in the previous experiment using 1aΔCT and 1bΔCT, $1aNT_{tm}$ and $1bNT_{tm}$ did not bind when lysates individually expressing each construct were mixed (Fig. 2*D*, *lanes 3* and *4*).

Heteromeric N Termini of hERG1 Bind in a Direct Dose-dependent Manner—Attempts to demonstrate association of soluble N termini in the absence of TM were not successful because the short 1b N terminus failed to express in HEK-293 cells. Instead, we turned to *in vitro* binding assays to determine whether 1aNT and 1bNT polypeptides purified from *E. coli* could bind directly without the TM domains and the 30-aa region of homology in their N termini. We incubated 2 μM bead-bound GST-1bNT with increasing amounts of soluble 1aNT from 0.3 to 10 μM in separate reactions, eluted bound complex from the beads, and resolved the eluate using SDS-PAGE. Binding of 1aNT to GST-1bNT was sufficiently robust to be visualized by Coomassie Blue staining (Fig. 3*A*, *lanes 1–6*). The low efficiency of 1aNT binding is attributable to the large degree of degradation of 1bNT (visible on gel, under the indicated GST-1bNT polypeptide) and to competing homotypic association of 1aNT fragments (supplemental Fig. S1). Immobilized GST used as a negative control did not show binding to the 1a N terminus at any concentration used (Fig. 3*A*, *lanes 7–12*). A dose-response curve plotting the OD of soluble 1aNT bound to GST-1bNT as a function of 1aNT concentration shows binding occurs with an EC_{50} of 0.96 ± 0.2 μM and a Hill coefficient of 1.52 (Fig. 3*B*). These results indicate that the 1a and 1b N termini bind each other directly and thus potentially mediate association of heteromeric subunits during assembly.

Truncated hERG 1b Serves as a Reporter for Early ER Events—To determine whether hERG 1a and 1b N termini interactions play a role in biogenesis, we next sought an approach to perturb their interaction and measure the effect on early events in assembly. We discovered that the C-truncated construct 1bΔCT exists not in core and maturely glycosylated forms, as is the case for full-length 1b (24), but rather in core and unglycosylated forms (Fig. 4). We identified the core glycoform based on its sensitivity to both PNGase F and Endoglycosidase H (Endo H), which collapsed the 38-kDa 1bΔCT to the same size as the lower, unglycosylated band migrating at ~35 kDa (Fig. 4*A*). Fig. 4*B* shows mature, full-length hERG 1b is insensitive to Endo H, thus ensuring the specificity of the enzyme treatment. The presence of the core and unglycosylated species presented an opportunity to identify, via perturbation, early events leading up to core glycosylation (see below).

1a N-terminal Fragments Disrupt hERG1bΔCT Oligomerization—We exploited ER glycosylation of 1bΔCT to identify the role of heteromeric N-terminal interactions in early assembly of hERG channels. We hypothesized that core glycosylation might report oligomerization of 1bΔCT, and that disruption of these events by 1aNT fragments would provide evidence of heteromeric N-terminal interactions. We first tested

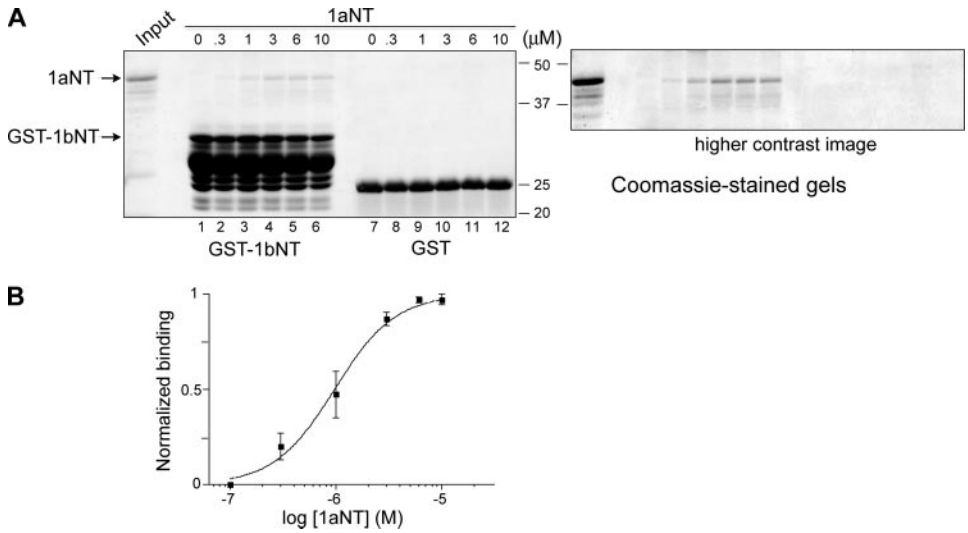

FIGURE 3. **hERG 1a and 1b N termini interact *in vitro*.** *A*, *left panel*, Coomassie Blue-stained gel showing direct interaction between 1a and 1b N termini. *Lanes 1–6*, co-sedimentation of 1aNT with immobilized GST-1bNT (*arrows*). Each reaction contained indicated amounts of soluble 1aNT-His_6. The amount of 1aNT bound to 1bNT was roughly 50–500 ng, falling within the sensitivity and linear range of the Coomassie Blue stain (64). 100 percent of bead-bound material was loaded. *Lanes 7–12*, soluble 1aNT does not co-sediment with GST alone. Each binding reaction has equal amounts of bead protein. Data shown are representative of three independent experiments. *Right panel*, a higher contrast image of the Coomassie Blue-stained gel in the *left panel*. *B*, optical density of the bound 1aNT (*upper arrow* in *A*) at each concentration (*lanes 1–6*) was divided by the corresponding GST-1bNT input (*lower arrow*) to control for loading. Each fractional OD for 1aNT was then normalized to the maximum (*lane 6*) and plotted against the concentration of soluble 1aNT.

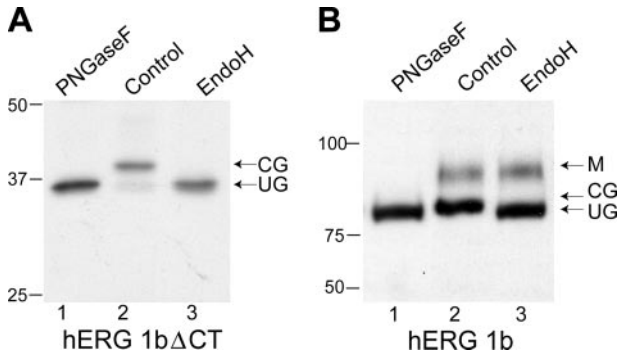

FIGURE 4. **C-terminal-truncated 1b reports core glycosylation.** *A*, Western blot probed with 1b-specific antibody shows 1bΔCT is reduced by both PNGase F (*lane 1*) and Endo H (*lane 3*) treatment. *B*, in contrast, full-length hERG 1b has a mature, Endo H-insensitive band as well as an Endo H-sensitive band. PNGase F removes all glycan groups from 1b. *Lane 2* in each case is the untreated lysate. *M*, mature; *CG*, core-glycosylated; *UG*, unglycosylated.

whether 1bΔCT subunits oligomerize by co-expressing 1bΔCT-Myc with 1bΔCT-GFP in HEK-293 cells. Using Myc antibodies, we found the larger 1bΔCT-GFP fusion protein co-immunoprecipitated with the 1bΔCT-Myc (Fig. 5*A*, *lanes 1* and *2*). The two species do not interact in mixed lysates from cells independently expressing the two constructs (Fig. 5*A*, *lanes 4* and *5*). Reciprocal immunoprecipitates using GFP antibodies gave similar results (data not shown).

If 1a and 1b N termini efficiently interact, we expect $1aNT_{tm}$ fragments to disrupt hERG1bΔCT homo-oligomerization. Indeed, as is evident from Western blot results, co-transfection with comparable amounts of $1aNT_{tm}$ (see supplemental Fig. S2) caused a significant reduction in homo-oligomerization (Fig. 5*A*, *lanes 6* and *7*). Association of 1bΔCT-Myc and 1bΔCT-GFP oligomers was dramatically reduced by 80 ± 13% ($p = 0.0011$, $n = 4$; Fig. 5*B*). Thus, the 1aNT fragment disrupts 1bΔCT oligomerization. These experiments demonstrate that avid interaction between 1a and 1b N termini mediate heteromeric assembly.

1a N-terminal Fragments Cause Accumulation of Unglycosylated 1bΔCT—The perturbation of 1bΔCT oligomerization could occur by one of two mechanisms: the $1aNT_{tm}$ fragment prevents 1b N-terminal interactions during biogenesis, or it causes dissociation of extant 1b oligomers. Preventing early assembly is expected to disrupt core glycosylation, whereas any disruption of preformed 1bΔCT oligomers is not. By measuring core glycosylation, we can pinpoint the timing of the $1aNT_{tm}$ and 1bΔCT interaction.

We cotransfected 1bΔCT into HEK-293 cells with one of the following constructs: empty vector (control), $1aNT_{tm}$, or NdeI (lacking N-terminal residues 1–354; cf. Fig. 1*A*). We assayed the effects of the disrupting fragments in 1bΔCT lysates by measuring the core glycoform as a fraction of the total (core-plus unglycosylated) signal. As compared with the control, cotransfection of 1bΔCT with $1aNT_{tm}$ resulted in significant reduction in core-glycosylated 1bΔCT, suggesting that the heteromeric N termini interacted prior to the glycosylation step ($p < 0.005$, $n = 3$; Fig. 6, *A* and *B*). NdeI also reduced core glycosylation but to a lesser extent ($p < 0.05$, $n = 3$), and we could not rule out whether this reduction was because of its competition for the glycosylation machinery. In contrast, the greater enrichment of unglycosylated 1bΔCT by $1aNT_{tm}$ could not have resulted from a direct exhaustion of the glycosylation machinery, because $1aNT_{tm}$ lacks the hERG1 *N*-linked glycosylation site. The $1aNT_{tm}$ fragment associated primarily with the unglycosylated 1bΔCT in co-immunoprecipitation experiments, indicating the increase in unglycosylated 1bΔCT was because of its direct physical association with the disrupting fragments (Fig. 6*C*). Together, the results above indicate that N-terminal interactions disrupt oligomerization and core glycosylation, reflecting early biogenic events.

Interaction with hERG 1a N Terminus Prevents Maturation of 1bΔCT—As an alternative explanation for the increase in abundance of unglycosylated 1bΔCT just described, we considered whether 1a N-terminal fragments might promote degradation of 1bΔCT rather than prevent core glycosylation. If so, we would expect to see an accumulation of deglycosylated 1bΔCT species in the cytosol en route to degradation as part of the unfolded protein response (35, 36). We used pulse chase labeling to test this possibility. We co-transfected 1bΔCT with vector (as a control) or with $1aNT_{tm}$ fragment in HEK-293 cells. We radiolabeled cells for 5 min, and immunoprecipitated

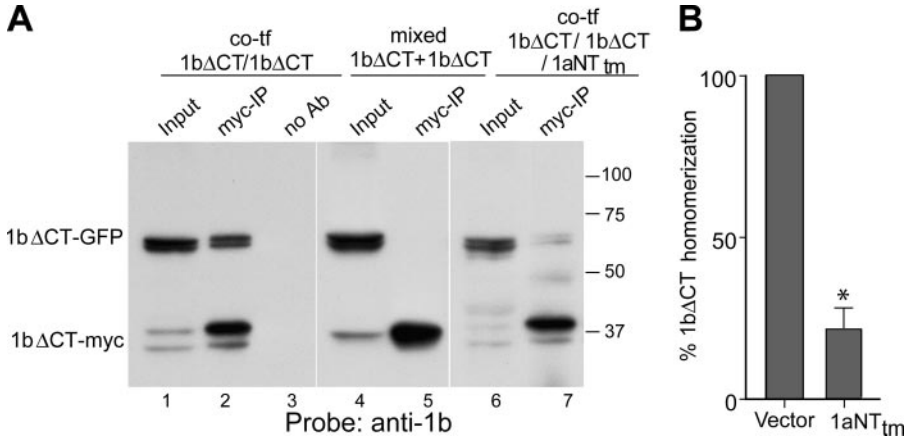

FIGURE 5. **Truncated 1b subunits homo-oligomerize and 1aNT$_{tm}$ reduces this oligomerization.** *A*, Western blot probed with 1b-specific antibody. *Lane 1*, lysate from cells co-expressing 1bΔCT-GFP and 1bΔCT-Myc. Similar to 1bΔCT-Myc, 1bΔCT-GFP expresses as a doublet. *Lanes 2* and *3*, 25% of the eluate from lysate shown in *lane 1*, precipitated with or without anti-Myc, respectively. *Lanes 4* and *5*, input and IP from mixed lysate individually expressing the tagged constructs show no association. *Lanes 6* and *7*, input and 25% IP eluate from lysate co-expressing 1bΔCT-GFP, 1bΔCT-Myc, and 1aNT$_{tm}$. Input lanes represent 5% (25 μg) of the total lysate used for each IP. The expression level of 1aNT$_{tm}$ was comparable to that of 1bΔCT constructs (see supplemental Fig. S2). *B*, degree of 1bΔCT-GFP and 1bΔCT-Myc oligomerization in the absence or presence of 1aNT$_{tm}$ was determined by measuring the OD of the 1bΔCT-GFP and 1bΔCT-Myc bands in *lanes 1*, *2*, *6*, and *7* (also see "Experimental Procedures").

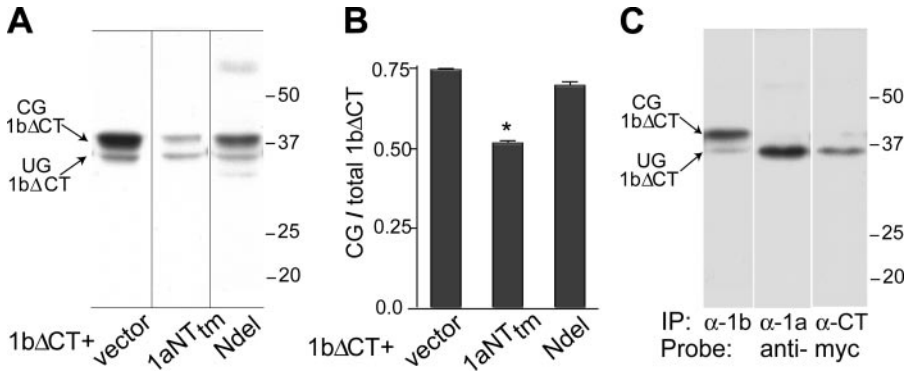

FIGURE 6. **hERG 1a N-terminal fragments reduce fraction of core-glycosylated/total 1bΔCT.** *A*, Western blots of lysates co-expressing 1bΔCT-Myc and vector (control, *lane 1*), 1aNT$_{tm}$ (*lane 2*), or NdeI (*lane 3*), probed with 1b-specific antibodies. *B*, densitometric readings were obtained for the core-glycosylated and unglycosylated 1bΔCT proteins bands in each lysate. *Error bars* represent S.E. from three independent trials. *C*, Western blot of IP eluates from each lysate (1bΔCT with vector, 1aNTtm, or NdeI) was probed with Myc antibody to detect coprecipitated 1bΔCT. A representative example of three independent trials is shown.

expressed polypeptides from the cell lysate. The 1bΔCT protein in mock-transfected cells manifests as both the unglycosylated and more abundant core-glycosylated forms (Fig. 7*A*, *left panel*). In the presence of 1aNT$_{tm}$, the core-glycosylated 1bΔCT never appeared, even as early as the transition between the 5-min pulse period and the beginning of the chase period (Fig. 7*A*, *right panel*). Endo H selectively reduced the upper 1bΔCT band in control cells, confirming its identity as the core glycoform (Fig. 7*B*). The rapidity with which association of 1aNT$_{tm}$ caused a loss of the core glycosylated band suggests 1aNT$_{tm}$ prevented core glycosylation of nascent 1bΔCT, rather than promoting deglycosylation of mature 1bΔCT en route to degradation. Fractionation studies in a stable 1bΔCT cell line further support this conclusion by showing that unglycosylated 1bΔCT is associated with 1aNT$_{tm}$ in the membrane fractions rather than the cytosol (see supplemental data). The perturbation of cotranslational glycosylation confirms that 1a and 1b N termini associate early, prior to the core glycosylation of the S5-P linker as it emerges from the translocon.

DISCUSSION

In the current study, we investigated the biochemical basis for heteromeric assembly of hERG1 channels during biogenesis. We showed that hERG 1a and 1b subunits assemble in the ER. Their N termini interact *in vitro* in a direct and dose-dependent manner. As illustrated in the model in Fig. 8, the 1a N-terminal fragment interacts with the 1b N terminus and prevents oligomerization of a truncated 1b construct (1bΔCT). Cotranslational glycosylation of 1bΔCT is concomitantly reduced, suggesting heteromeric N termini interact prior to glycosylation and therefore cotranslationally. Heteromeric interaction and inhibition of glycosylation occurred within 5 min of the onset of protein synthesis as measured with pulse chase. Thus, N-terminal interactions are crucial to early assembly in the biogenesis of hERG1 channels.

Mechanisms controlling homo- and hetero-multimeric assembly of membrane proteins have been explored in several other systems. In the distantly related Shaker Kv channels, homo-oligomerization is facilitated by the association of homologous tetramerizing (T1) interaction domains (22, 37, 38). Nascent N-terminal T1 domains interact cotranslationally, associating as they are produced on the ribosome and well before the pore-forming domains have been synthesized or properly folded (23, 39–41). The efficiency of this process depends on the presence of the ER membrane, which is thought to concentrate the interacting domains that would otherwise be diluted in the cytosol (20, 41). Moreover, the transmembrane anchors facilitate the appropriate folding of the contiguous N terminus (42–46). The interaction of the T1 domains is also thought to regulate heteromeric assembly: channels from divergent Kv subfamilies (*e.g.* Kv1.1, Kv2.1) can assemble, albeit inefficiently, only if their T1 domains have been removed (47); if the T1 domains are present, only heteromers from within a subfamily (*e.g.* Kv1.1, Kv1.3) will be produced (48). In contrast to Kv and ligand-gated channels, where oligomerization occurs via the interactions of homologous N termini (19, 21, 49, 50), our results indicate the assembly of hERG 1a and 1b proceeds by the interaction of structurally dissimilar domains.

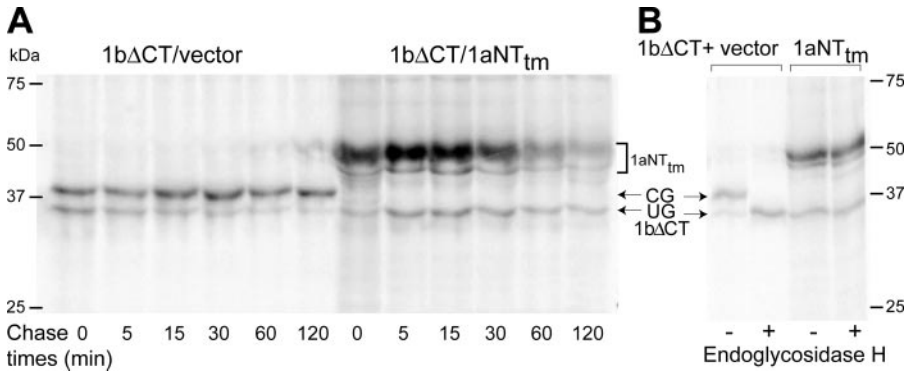

FIGURE 7. **Interaction with 1aNT$_{tm}$ prevents maturation of 1bΔCT.** *A*, scanned image from a phosphorimager screen showing radiolabeled 1bΔCT in the absence or presence of 1aNT$_{tm}$ captured at different time points. In addition to 1bΔCT bands, 1aNT$_{tm}$ protein is also detected in the latter. *B*, scanned phosphorimage of Endo H-treated and untreated 1bΔCT+pcDNA3.1 and 1bΔCT+1aNT$_{tm}$ radiolabeled lysates confirms identity of 1bΔCT bands observed in Fig. 7*A*.

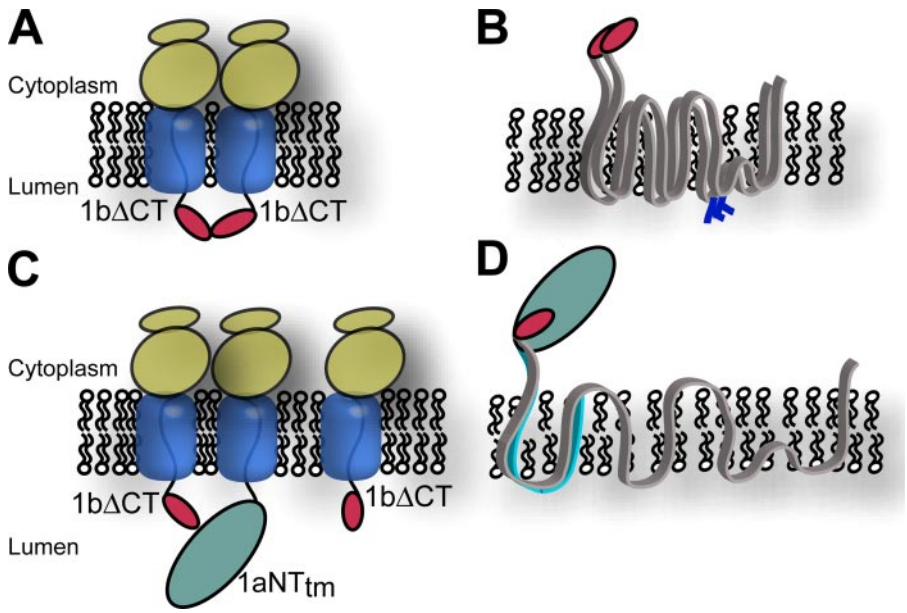

FIGURE 8. **Model showing preferential heteromeric association with 1a N terminus prevents homo-oligomerization of 1bΔCT and interferes with cotranslational glycosylation.** *A*, two 1bΔCT polypeptides (N termini in *red*) interact as they emerge from the translocon (*blue*) while they are being translated on the ribosomes (*yellow*). *B*, properly assembled and folded 1bΔCT subunits are flipped to allow for cotranslational glycosylation (inverted *blue Y*) between the S5 and P-loop in the ER lumen. *C*, in the presence of the 1aNT$_{tm}$ (*green*), cotranslational association between the heteromeric N termini prevents the homotypic 1bΔCT interaction. *D*, improperly assembled subunits fail to core glycosylate.

Why glycosylation is disrupted in the presence of heteromerizing N termini is not known. The hERG subunit has a single glycosylation site, and the core glycosylation machinery may require a double glycan moiety not present in the 1bΔCT-1aNT$_{tm}$ complex. Alternatively, failure to fully oligomerize or global folding disturbances may reduce accessibility to the core glycosylation machinery. The heteromerizing fragment may also prevent topological changes that allow exposure of the glycosylation site to the lumen.

A tangential but important result from this experiment is that truncation of the C terminus results in accumulation of the core glycoform and reveals a requirement for the C terminus in Golgi-mediated hERG 1b glycosylation. Expression of 1aΔCT gave similar results (supplemental Fig. S3), indicating that the hERG1 C terminus is of general importance in Golgi-mediated glycosylation. We speculate that the absence of the C terminus deprives truncated hERG1 proteins of interactions with forward trafficking partners that ensure their arrival at the Golgi. Alternatively, C-terminal truncation may prevent interaction with proteins normally required to detain hERG1 in the Golgi long enough to ensure appropriate glycosylation (54, 55). Golgi-mediated glycosylation of hERG1 channels is not a requirement for function or trafficking but it does enhance channel stability (28). Therefore, indirectly the C terminus may play a critical role in channel stability.

Whether hERG 1a channels have an N-terminal oligomerization domain similar to T1 remains controversial. A hERG 1a N-terminal fragment termed NAB associates as tetramers in solution (51), whereas in crystal structures the same protein fragment exists strictly as monomers (52). Although crystallography also revealed a PAS domain predicted to be involved in protein-protein interactions (53), the specific 1a N-terminal domains mediating heteromeric association remain to be determined.

The perturbation of 1bΔCT oligomerization by the 1aNT$_{tm}$ fragment indicates the 1b N termini interact cotranslationally during homo-oligomerization. This result was not necessarily predicted from analysis of the short, 36-amino acid 1b N terminus, which exhibits an excess of 8 positively charged residues. Our results indicate these charges do not present an electrostatic barrier to 1b N-terminal homo-oligomerization.

Recent studies have established the 1b subunit as an important component of heteromeric hERG1 channels in cardiac as well as neoplastic tissues (24, 56, 57). hERG1 channels have been implicated in cell proliferation and invasiveness, where their ectopic or enhanced expression imparts a growth advantage to cancerous cells (6, 58–61). In several tumor cells, such as neuroblastomas and leukemias, both 1a and 1b subunits are present as heteromeric populations (56). This heteromeric assembly, facilitated by early N-terminal interactions, may be a critical determinant of interaction with other protein partners and subcellular localization of hERG1 channels. For instance, β_1 integrin interacts selectively with hERG 1a and not hERG 1b in neuroblastoma cell lines, where it triggers signaling cascades important in cell proliferation, adhesion, and migration (62).

The presence of 1b might regulate 1a N-terminal interactions with the β_1 integrin and in turn determine the localization of hERG 1a/β_1 integrin complexes in caveolae-containing lipid rafts.

hERG1 channels have been intensively studied because of their role as a target for LQTS. Trafficking defects have been identified as a major mechanism underlying congenital LQTS (10, 63). Unraveling the assembly process may provide clues to the varied mechanisms by which hERG1 mutations, many of which are unique to the 1a N terminus, can result in LQTS. Mutations could reduce the efficiency of heteromeric hERG1 channel assembly, or mediate dominant-negative interactions between 1a and 1b subunits, resulting in ER retention, enhanced degradation, reduced surface expression and lower current magnitudes, all processes capable of reducing repolarizing current and causing LQTS. Additionally, C-terminal mutations could interfere with complex glycosylation thereby destabilizing channels at the cell surface and potentially reducing hERG1 current.

In summary, our results demonstrate that the N termini interact in a direct, dose-dependent manner and mediate heteromeric association of hERG1 subunits during channel biogenesis. This interaction, which takes place between structurally divergent N-terminal domains of the respective 1a and 1b subunits, is a critical step in the assembly of this unique channel.

Acknowledgments—We thank members of the Robertson laboratory and Drs. Andrew Boileau, Akhil Bhalla, Edwin Chapman, Cynthia Czajkowski, Timothy Kamp, and Jeffery Walker for helpful discussions.

REFERENCES

1. Ohya, S., Horowitz, B., and Greenwood, I. (2002) *Am. J. Physiol. Cell Physiol* **283,** C866–C877
2. Farrelly, A. M., Ro, S., Callaghan, B. P., Khoyi, M. A., Fleming, N., Horowitz, B., Sanders, K. M., and Keef, K. D. (2003) *Am. J. Physiol. Gastrointest Liver Physiol.* **284,** G883–G895
3. Arcangeli, A. (2005) *Novartis Found Symp.* **266,** 225–232
4. Sanguinetti, M. C., Jiang, C., Curran, M. E., and Keating, M. T. (1995) *Cell* **81,** 299–307
5. Trudeau, M. C., Warmke, J. W., Ganetzky, B., and Robertson, G. A. (1995) *Science* **269,** 92–95
6. Pillozzi, S., Brizzi, M., Balzi, M., Crociani, O., Cherubini, A., Guasti, L., Bartolozzi, B., Becchetti, A., Wanke, E., Bernabei, P., Olivotto, M., Pegoraro, L., and Arcangeli, A. (2002) *Leukemia* **16,** 1791–1798
7. Gullo, F., Ales, E., Rosati, B., Lecchi, M., Masi, A., Guasti, L., Cano-Abad, M., Arcangeli, A., Lopez, M., and Wanke, E. (2003) *Faseb J.* **17,** 330–332
8. Fitzgerald, P. T., and Ackerman, M. J. (2005) *Heart Rhythm* **2,** Suppl. 2, S30–S37
9. Curran, M. E., Splawski, I., Timothy, K. W., Vincent, G. M., Green, E. D., and Keating, M. T. (1995) *Cell* **80,** 795–803
10. Zhou, Z., Gong, Q., Epstein, M. L., and January, C. T. (1998) *J. Biol. Chem.* **273,** 21061–21066
11. Zhou, Z., Gong, Q., and January, C. T. (1999) *J. Biol. Chem.* **274,** 31123–31126
12. Furutani, M., Trudeau, M. C., Hagiwara, N., Seki, A., Gong, Q., Zhou, Z., Imamura, S., Nagashima, H., Kasanuki, H., Takao, A., Momma, K., January, C. T., Robertson, G. A., and Matsuoka, R. (1999) *Circulation* **99,** 2290–2294
13. Ficker, E., Dennis, A. T., Obejero-Paz, C. A., Castaldo, P., Taglialatela, M., and Brown, A. M. (2000) *J. Mol. Cell Cardiol.* **32,** 2327–2337
14. Ficker, E., Thomas, D., Viswanathan, P. C., Dennis, A. T., Priori, S. G., Napolitano, C., Memmi, M., Wible, B. A., Kaufman, E. S., Iyengar, S., Schwartz, P. J., Rudy, Y., and Brown, A. M. (2000) *Am. J. Physiol. Heart Circ. Physiol.* **279,** H1748–H1756
15. January, C. T., Gong, Q., and Zhou, Z. (2000) *J. Cardiovasc. Electrophysiol.* **11,** 1413–1418
16. Ellgaard, L., and Helenius, A. (2003) *Nat Rev Mol. Cell. Biol.* **4,** 181–191
17. Robertson, G. A., and January, C. T. (2006) *Handb. Exp. Pharmacol.* **171,** 349–355
18. Rajamani, S., Anderson, C. L., Anson, B. D., and January, C. T. (2002) *Circulation* **105,** 2830–2835
19. Deutsch, C. (2003) *Neuron* **40,** 265–276
20. Shahla, V., and Zach, W. H. (1992) *Cell* **68,** 23–31
21. Deal, K. K., Lovinger, D. M., and Tamkun, M. M. (1994) *J. Neurosci.* **14,** 1666–1676
22. Li, M., Jan, Y., and Jan, L. (1992) *Science* **257,** 1225–1230
23. Lu, J., Robinson, J. M., Edwards, D., and Deutsch, C. (2001) *Biochemistry* **40,** 10934–10946
24. Jones, E. M., Roti Roti, E. C., Wang, J., Delfosse, S. A., and Robertson, G. A. (2004) *J. Biol. Chem.* **279,** 44690–44694
25. London, B., Trudeau, M. C., Newton, K. P., Beyer, A. K., Copeland, N. G., Gilbert, D. J., Jenkins, N. A., Satler, C. A., and Robertson, G. A. (1997) *Circ. Res.* **81,** 870–878
26. Lees-Miller, J. P., Kondo, C., Wang, L., and Duff, H. J. (1997) *Circ. Res.* **81,** 719–726
27. Jordan, M., and Wurm, F. (2004) *Methods* **33,** 136–143
28. Gong, Q., Anderson, C. L., January, C. T., and Zhou, Z. (2002) *Am. J. Physiol. Heart Circ. Physiol.* **283,** H77–H84
29. Helenius, A., and Aebi, M. (2004) *Annu. Rev. Biochem.* **73,** 1019–1049
30. Rothman, J., and Lodish, H. (1977) *Nature* **269,** 775–780
31. Chen, W., Helenius, J., Braakman, I., and Helenius, A. (1995) *Proc. Natl. Acad. Sci. U. S. A.* **92,** 6229–6233
32. Kornfeld, R., and Kornfeld, S. (1985) *Annu. Rev. Biochem.* **54,** 631–664
33. Zhou, Z., Gong, Q., Ye, B., Fan, Z., Makielski, J. C., Robertson, G. A., and January, C. T. (1998) *Biophys. J.* **74,** 230–241
34. Jenke, M., Sanchez, A., Monje, F., Stuhmer, W., Weseloh, R. M., and Pardo, L. A. (2003) *EMBO J.* **22,** 395–403
35. Kopito, R. R. (1997) *Cell* **88,** 427–430
36. Gong, Q., Keeney, D. R., Molinari, M., and Zhou, Z. (2005) *J. Biol. Chem.* **280,** 19419–19425
37. Shen, N. V., and Pfaffinger, P. J. (1995) *Neuron* **14,** 625–633
38. Xu, J., Yu, W., Jan, Y. N., Jan, L. Y., and Li, M. (1995) *J. Biol. Chem.* **270,** 24761–24768
39. Lu, J., and Deutsch, C. (2001) *Biochemistry* **40,** 13288–13301
40. Deutsch, C. (2002) *Annu. Rev. Physiol.* **64,** 19–46
41. Kosolapov, A., and Deutsch, C. (2003) *J. Biol. Chem.* **278,** 4305–4313
42. Babila, T., Moscucci, A., Wang, H., Weaver, F., and Koren, G. (1994) *Neuron* **12,** 615–626
43. Tu, L., Santarelli, V., and Deutsch, C. (1995) *Biophys. J.* **68,** 147–156
44. Lu, Y., Xiong, X., Helm, A., Kimani, K., Bragin, A., and Skach, W. R. (1998) *J. Biol. Chem.* **273,** 568–576
45. Tu, L., Wang, J., Helm, A., Skach, W. R., and Deutsch, C. (2000) *Biochemistry* **39,** 824–836
46. Sato, Y., Sakaguchi, M., Goshima, S., Nakamura, T., and Uozumi, N. (2002) *Proc. Natl. Acad. Sci. U. S. A.* **99,** 60–65
47. Lee, T. E., Philipson, L. H., Kuznetsov, A., and Nelson, D. J. (1994) *Biophys. J.* **66,** 667–673
48. Covarrubias, M., Vyas, T. B., Escobar, L., and Wei, A. (1995) *J. Biol. Chem.* **270,** 19408–19416
49. Nagaya, N., and Papazian, D. M. (1997) *J. Biol. Chem.* **272,** 3022–3027
50. Green, W. N. (1999) *J. Gen. Physiol.* **113,** 163–170
51. Li, X., Xu, J., and Li, M. (1997) *J. Biol. Chem.* **272,** 705–708
52. Morais Cabral, J. H., Lee, A., Cohen, S. L., Chait, B. T., Li, M., and Mackinnon, R. (1998) *Cell* **95,** 649–655
53. Pellequer, J.-L., Wager-Smith, K. A., Kay, S. A., and Getzoff, E. D. (1998) *Proc. Natl. Acad. Sci. U. S. A.* **95,** 5884–5890
54. Kupershmidt, S., Snyders, D. J., Raes, A., and Roden, D. M. (1998) *J. Biol.*

Chem. **273,** 27231–27235
55. Roti Roti, E. C., Myers, C. D., Ayers, R. A., Boatman, D. E., Delfosse, S. A., Chan, E. K., Ackerman, M. J., January, C. T., and Robertson, G. A. (2002) *J. Biol. Chem.* **277,** 47779–47785
56. Crociani, O., Guasti, L., Balzi, M., Becchetti, A., Wanke, E., Olivotto, M., Wymore, R. S., and Arcangeli, A. (2003) *J. Biol. Chem.* **278,** 2947–2955
57. Lees-Miller, J. P., Guo, J., Somers, J. R., Roach, D. E., Sheldon, R. S., Rancourt, D. E., and Duff, H. J. (2003) *Mol. Cell. Biol.* **23,** 1856–1862
58. Arcangeli, A., Bianchi, L., Becchetti, A., Faravelli, L., Coronnello, M., Mini, E., Olivotto, M., and Wanke, E. (1995) *J. Physiol.* **489,** 455–471
59. Bianchi, L., Wible, B., Arcangeli, A., Taglialatela, M., Morra, F., Castaldo, P., Crociani, O., Rosati, B., Faravelli, L., Olivotto, M., and Wanke, E. (1998) *Cancer Res.* **58,** 815–822
60. Smith, G. A. M., Tsui, H.-W., Newell, E. W., Jiang, X., Zhu, X.-P., Tsui, F. W. L., and Schlichter, L. C. (2002) *J. Biol. Chem.* **277,** 18528–18534
61. Arcangeli, A., Becchetti, A., Cherubini, A., Crociani, O., Defilippi, P., Guasti, L., Hofmann, G., Pillozzi, S., Olivotto, M., and Wanke, E. (2004) *Biochem. Soc Trans.* **32,** 826–827
62. Cherubini, A., Hofmann, G., Pillozzi, S., Guasti, L., Crociani, O., Cilia, E., Di Stefano, P., Degani, S., Balzi, M., Olivotto, M., Wanke, E., Becchetti, A., Defilippi, P., Wymore, R., and Arcangeli, A. (2005) *Mol. Biol. Cell* **16,** 2972–2983
63. Anderson, C. L., Delisle, B. P., Anson, B. D., Kilby, J. A., Will, M. L., Tester, D. J., Gong, Q., Zhou, Z., Ackerman, M. J., and January, C. T. (2006) *Circulation* **113,** 365–373
64. Wirth, P. J., and Romano, A. (1995) *J. Chromatogr. A* **698,** 123–143